THE SECOND HINODE SCIENCE MEETING
ASP Conference Series, Vol. 415, ©2009
B. Lites, M. Cheung, T. Magara, J. Mariska, and K. Reeves

MULTI3D: A Domain-Decomposed 3D Radiative Transfer Code

Jorrit Leenaarts and Mats Carlsson

Institute for Theoretical Astrophysics, University of Oslo
Center of Mathematics for Applications, University of Oslo

Abstract. We present MULTI3D, a 3D radiative transfer code currently under development. It is optimized for computing NLTE problems based on (radiation-)MHD models of stellar atmospheres. MULTI3D is based on MULTI and includes most of the physics present in that code. MULTI3D was first written as a serial code by Botnen (1997) and has recently been upgraded to an MPI-parallelized, domain-decomposed version. The code has so far successfully been run on up to 64 processors, solving the NLTE radiative transfer for a six-level Ca II atom with 400 frequency points in an atmosphere of 256 x 128 x 108 grid points.

1. The Code

In recent years, it has become possible to perform three-dimensional radiation-magneto-hydro-dynamic simulations of the solar chromosphere. These simulations give quantities such as temperatures, densities, and magnetic field strengths as output. These can, however, not directly be compared to observations. First, one has to translate the model parameters to emergent intensities in the spectral lines of interest.

Chromospheric spectral lines form in general in NLTE and require computation of the three-dimensional radiation field. Because of the large number of spatial, angle and frequency points this is a computationally intensive task.

We present MULTI3D, a domain-decomposed MPI-parallelized code that efficiently solves the NLTE radiative transfer problem in 3D Cartesian geometry. It is based on the 1D code MULTI (Carlsson 1986) and a serial version of MULTI3D developed by Botnen (1997). The code employs the complete linearization method of Scharmer and Carlsson (1985) to solve NLTE problems in 3D geometry. Scattering in lines is treated in complete redistribution while background scattering is coherent. Overlapping transitions are not allowed. Collisional-radiative switching and convergence acceleration are implemented.

1.1. Short Characteristics

The code employs a 3D short characteristics solver for the radiation. It uses second-order Bezier interpolation for the source function, ensuring a positive source function along the characteristics. The radiation is not propagated throughout the whole computational domain per iteration. Instead, it is propagated over a small (typically 2) number of sub-domains per iteration. This means the average radiation field at a given point lags behind several iterations, but will converge to the correct solution when the corrections to the populations

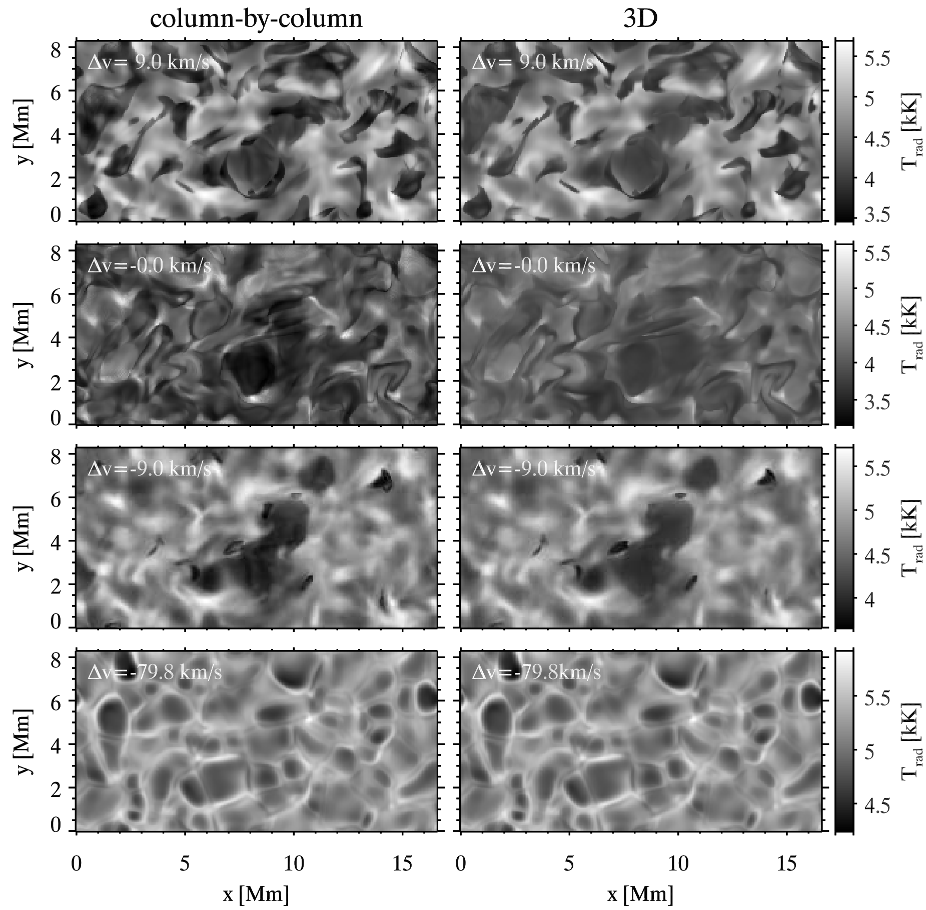

Figure 1. Emergent vertical intensity of the Ca II H line at 396.8 nm. Left-hand column: using a 1D column-by-column solver. Right-hand-column: using the 3D short-characteristic solver. Different rows are at different shifts from the line center indicated at the top left of each row, with positive velocities indicating a redshift. Each row has its own brightness scale indicated at the right. 3D effects become important close to the line core (first three rows), causing a decrease in contrast and occasionally completely washing out a feature (such as the dark spot at $(x, y) = (9, 5)$ Mm in the top-left panel, which is not present in the top-right panel). The bottom row shows LTE-formed reversed granulation, and the column-by-column and 3D images are indistinguishable.

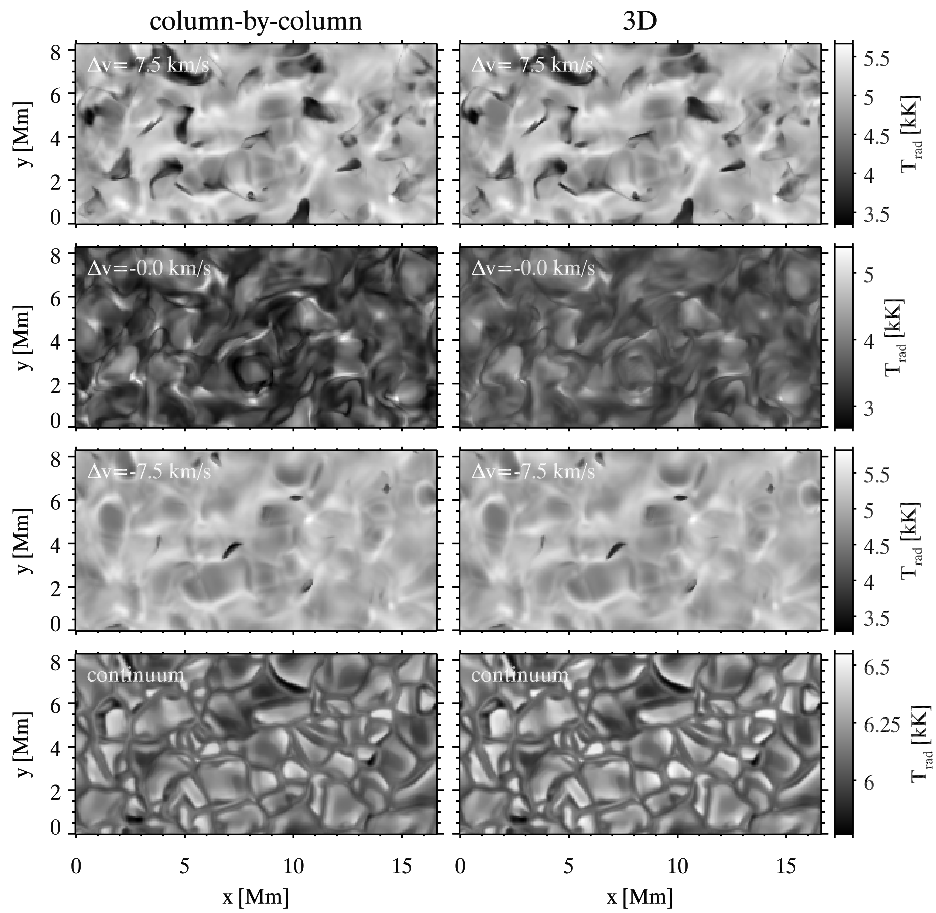

Figure 2. Emergent vertical intensity of the Ca II IR line at 854.2 nm. Left-hand column: using a 1D column-by-column solver. Right-hand-column: using the 3D short-characteristic solver. Different rows are at different shifts from the line center indicated at the top left of each row, with positive velocities indicating a redshift. Each row has its own brightness scale indicated at the right. 3D effects become important closer to the line core than in the case of Ca II H. The images at +7.5 and −7.5 km/s do not yet show a decrease in contrast, but in the line core the decrease is appreciable. The dark circular structure at around $(x, y) = (8, 3)$ Mm in the left-hand column is completely invisible in the 3D case.

become small. This solver ensures a speedup of the code linear with the number of processors N. In contrast, the speedup of a solver that propagates the radiation throughout the computational domain scales as $N^{2/3}$.

1.2. Memory Usage

3D NLTE radiative transfer codes are very memory intensive. MULTI3D needs to store the average radiation field for each frequency and the intensity at the sub-domain boundaries for each frequency and angle between iterations. This amounts to 1GB of memory per sub-domain for a sub-domain size of $32 \times 32 \times 32$, 600 frequency and 24 angle points. This is small enough to fit into memory on today's supercomputers. If the problem demands more memory the persistent data can be written to file between iterations. This provides the possibility of solving the radiative transfer problem for atoms with a large number of transitions at the penalty of decreased performance.

1.3. Test Computation

We performed a test computation on a snapshot of the radiative-MHD simulation of flux emergence by Martínez-Sykora et al. (2008). The computational domain for the radiative transfer computation had $256 \times 128 \times 108$ grid points. We used a 5-level-plus-continuum Ca II atom with 400 frequency points and treated the ray quadrature with 24 angles. The computation ran on 64 processors and took one day. Figures 1 and 2 compare the vertical emergent intensity of the Ca II H and 854.2 nm IR lines to computations where each column of the atmosphere is treated as plane-parallel. 3D effects become important close to the line core and tend to decrease the RMS contrast. They also occasionally wash out smaller features visible in the column-by-column computation because the radiation field that sets the NLTE source function is averaged over many adjacent locations.

The dark features visible in the first and third row of Figs. 1 and 2 are formed higher than the brighter background and are caused by strong upflows and downflows in the upper chromosphere shifting the line core out of the rest-wavelength.

2. Conclusions

We have shown early results of a 3D NLTE radiative transfer code that can solve the radiative transfer problem in snapshots of radiation-MHD simulations of the solar chromosphere. It is MPI-parallelized and its speedup scales linearly with the number of processors. We have tested it on a small test atmosphere; in the future we aim to use it to solve problems on atmospheres with a much larger number of grid points.

References

Botnen A., 1997, Master's thesis, University of Oslo
Carlsson M., 1986, Uppsala Astronomical Observatory Reports 33
Martínez-Sykora J., Hansteen V., Carlsson M., 2008, ApJ 679, 871
Scharmer G. B., Carlsson M., 1985, Journal of Computational Physics 59, 56